Frontiers in Bioscience Landmark

Front. Biosci. (Landmark Ed) **2025**; 30(6): 38830
https://doi.org/10.31083/FBL38830

Original Research

Functional Verification and Prognostic Value of Neutrophil Extracellular Trap-Related Genes in Pancreatic Cancer Progression

Jiaxin Xu[1,2,†], Liying Tu[1,2,†], Lijing Ma[1,2], Qisheng Tang[1,2], Yu Cao[1,2], Lihong Jiang[1,2,*]

[1]Faculty of Life Science and Technology, Kunming University of Science and Technology, 650500 Kunming, Yunnan, China
[2]Regenerative Medicine Research Center, The First People's Hospital of Yunnan Province, 650032 Kunming, Yunnan, China
*Correspondence: prof_jiang_khyy@163.com (Lihong Jiang)
[†]These authors contributed equally.
Academic Editor: Amedeo Amedei
Submitted: 5 March 2025 Revised: 2 May 2025 Accepted: 22 May 2025 Published: 26 June 2025

Abstract

Background: Pancreatic carcinoma (PC), a severely malignant neoplasm of the digestive system, is characterized by an unfavorable prognosis. Neutrophil extracellular trap (NETosis) is a neutrophilic inflammatory form of cell death. However, it is still unknown how they relate to one another. This study aims to explore the part NETosis plays in the onset and progression of pancreatic cancer. **Methods**: Expression and clinical data for patients with pancreatic carcinoma were obtained from publicly accessible databases. Multigene features were constructed using the least absolute shrinkage and selection operator (LASSO). Bioinformatics analysis was combined with *in vitro* experiments to determine the relevant mechanism. **Results**: Seventeen NETosis-related genes were identified. LASSO analysis finally led to the generation of six gene characteristics, which were divided into two clusters according to the expression level. The survival outcomes of the high- and low-risk groups differ significantly, and their predictive performance is good ($p < 0.05$). Drug sensitivity analysis confirmed that the high-risk cohort could benefit more from 5-fluorouracil, gemcitabine, and epirubicin ($p < 0.01$). Using survival analysis and single-cell binding quantitative real-time polymerase chain reaction (RT-qPCR), the crucial gene *LGALS3* was identified ($p < 0.0001$). *In vitro* experiments demonstrated that inhibiting *LGALS3* expression may significantly decrease the proliferation and movement of PANC-1 and SW1990 cells ($p < 0.05$). **Conclusion**: We established a 6-gene risk scoring model and confirmed the effect of *LGALS3* on the development of PC.

Keywords: pancreatic carcinoma; NETosis; LASSO; scRNA; LGALS3

1. Introduction

Pancreatic carcinoma is a highly aggressive neoplasm within the gastrointestinal tract. Clinically, pancreatic ductal adenocarcinoma, acinar cell carcinoma, small gland carcinoma, large eosinophilic granulocyte carcinoma, and small cell carcinoma are included in the pathological category of pancreatic carcinoma [1]. Presently, pancreatic carcinoma (PC) ranks as the fourth primary contributor to cancer-related deaths across the globe. By 2030, it is predicted to overtake all other malignant tumors as the leading cause of death worldwide [2]. In clinical practice, carbohydrate antigen 199 (CA19-9) is often considered a biomarker for the identification of PC. However, it has also been found to be elevated in benign and malignant digestive system disorders to various degrees, has poor specificity, and cannot be used as a screening tool [3]. Most individuals diagnosed with pancreatic cancer do not exhibit any symptoms during the initial stages of the disease, thereby decreasing their 5-year survival rate [4]. Currently, gemcitabine- or 5-fluorouracil-based chemotherapy is typically used in conjunction with surgery to treat PC [5]. Even with advancements in radiation and chemotherapy, the patient survival rate for PC has remained extremely low in recent years [6]. Immunotherapy, targeted treatment, and evidence-based dietary therapies have improved the prognosis of some patients affected by malignant tumors, such as those with PC with high microsatellite instability/mismatch repair errors [7,8]. However, the safety of these medications, particularly with respect to liver damage, is a concern that should not be overlooked [9]. The extraordinarily complex genetic landscape of PC significantly influences the formation of tumor microenvironments, encouraging tumor growth, treatment resistance, and immune escape mechanisms [10]. Consequently, the occurrence and progression of pancreatic cancer have become major global public health issues, and it is imperative to determine the role immune cells play in this process.

Neutrophil extracellular trap (NETosis) is a unique mechanism of neutrophil death, which was first recognized as an immunological response to bacterial infections [11]. After engulfing pathogens, the secretion of particles containing cytotoxic enzymes can achieve host defense [12]. A number of recent research endeavors have indicated that neutrophils, along with trapping nets, contribute to the process of carcinogenesis by indirectly causing deoxyribonucleic acid (DNA) damage through inflammation and di-

rectly enhancing the tumor microenvironment [13]. Revealing novel cell death pathways in malignant tumors and their molecular underpinnings provides a prospective therapeutic approach for the specific treatment of cancerous tumors. In this study, we assessed the predictive significance of NETosis by identifying distinct cluster features in a cohort from The Cancer Genome Atlas (TCGA). In addition, we investigated the relationship between the risk score and both overall survival and immune infiltration among patients diagnosed with PC. Based on this analysis, it is possible to enhance early detection, prognosis tracking, and individualized care for these patients.

2. Materials and Methods

2.1 Acquisition of the PC Dataset and the Genes Linked to NETosis

The transcriptome dataset GSE16515 comprising 52 patients with pancreatic cancer was obtained from the Gene Expression Omnibus (GEO) dataset (https://www.ncbi.nlm.nih.gov/gds/), The Gene Expression Omnibus Repository(GEO2R) tool was employed to pinpoint genes that are differentially expressed (DEGs). Using the GEIPA 2 website (http://gepia2.cancer-pku.cn/), we obtained differentially expressed genes of the The Cancer Genome Atlas - Pancreatic Adenocarcinoma (TCGA-PAAD) dataset. The GSE154778 dataset was used as the source of the single-cell dataset. Genes linked to NETosis were retrieved from the Gene Card (https://www.genecards.org/). The training set is the TCGA-PAAD queue, while the verification set is the external data set GSE57495.

2.2 Creation of NETosis-Related Genes Signature

Venn map was used to obtain NETosis-related DEGs. Univariate Cox analysis was employed to select NETosis-related genes linked to prognosis. The final gene signature was established using least absolute shrinkage and selection operator (LASSO) analysis [14].

2.3 Validation of the NETosis-Related Prognostic Model

The predict function determines each sample's risk score based on the multivariate Cox model, and the median value is used to categorize the patients in the modeling and verification queue into groups with elevated risk and groups with reduced risk. To assess the disparities in the survival rates between the two cohorts, survival status was assessed using the Kaplan–Meier (KM) curve, and the receiver operating characteristic (ROC) curve was used to judge the prognostic model's efficacy [15].

2.4 Examination of Drug Sensitivity and Immune Infiltration in a Subset Cohort

We investigated the association between infiltrating immune function and patient risk scores and utilized GSEABase and Gene Set Variation Analysis (GSVA) packages to determine the abundance of sixteen distinct varieties of infiltrating immune cells in both the high-risk and low-risk groups. The sensitivity of 196 medications was assessed for each patient risk group via the "oncoPredict" [16] package, a tool used for drug sensitivity prediction. The "calcPhenotype" function, which was trained using two datasets, GDSC2_Expr and GDSC2_Res, was used to forecast drug sensitivity based on patient data.

2.5 NETosis-Related Genes Signature was Assessed Using Single-Cell RNA Sequencing Analysis

"Seurat", an R package, was used for processing single-cell RNA sequencing (scRNA-seq) data, reducing dimensionality, performing normalization, and checking data quality. Extreme gene expression levels (nfeature RNA $>$200 and nfeature RNA $<$5000) were eliminated. The t-distributed stochastic neighbor embedding (t-SNE) approach was applied to standardize and decrease the dimensions and cluster the expression data. In accordance with the CellMarker database, the cells were labeled and categorized.

2.6 Cells and Reagents

The human normal pancreatic duct epithelial cell line named HPDE6-C7 (STCC11108), along with the human pancreatic cancer cell lines PANC-1 (STCC11102) and SW1990 (FH0784), were procured from Servicebio and Fuheng biology. Vivacell was the supplier from which fetal calf serum and Dulbecco's Modified Eagle's Medium (C3113-0500) were procured. *LGALS3* human pre-designed siRNA (HY-RS07604, siRNA sequences are presented in Table 1) and Cell Counting Kit-8 (HY-K0301) were purchased from MedChemExpress. Lipofectamine2000 (11668-019) was purchased from Invitrogen. The Total RNA Extraction Kit (DP430) was purchased from Tiangen. SweScript All-in-One RT SuperMix for qPCR (G3337) and 2xUniversal Blue SYBR Green qPCR Master (G3326) are sourced from Servicebio. PCR primers were synthesized by Qingke Biologics, Inc.

2.7 Sh-LGALS3-siRNA Cell Line Construction

PANC-1 and SW1990 cells were cultured in DMEM + 10%FBS + 1%PS complete medium, 5% CO_2, and 37 ° constant temperature. PANC-1 and SW1990 cells that were in the log phase of growth were seeded into 6-well plates at a cell concentration of 1×10^5. When the cell confluence was about 50%, they were replaced with a serum-free medium in which Lipofectamine2000 and Sh-*LGALS3*-siRNA plasmid were fully mixed at a ratio of 1:1. After the cells were treated for 6 hours, the serum-free medium was discarded and replaced with complete medium. The siRNA sequence with the highest interference effectiveness was chosen for further research after the total ribonucleic acid (RNA) was collected during 48 hours of continuous culture and the transfection efficiency was confirmed by reverse transcription quantitative real-time polymerase chain reaction (RT-

Table 1. siRNA sequences.

siRNA name	siRNA sequence
Negative Control-F	UUCUCCGAACGUGUCACGUTT
Negative Control-R	ACGUGACACGUUCGGAGAATT
LGALS3 Human Pre-designed siRNA Set A-1-F	GGGAAUUUCUGGUGACAUAUU
LGALS3 Human Pre-designed siRNA Set A-1-R	UAUGUCACCAGAAAUUCCCUU
LGALS3 Human Pre-designed siRNA Set A-2-F	GAGAACAACAGGAGAGUCAUU
LGALS3 Human Pre-designed siRNA Set A-2-R	UGACUCUCCUGUUGUUCUCUU
LGALS3 Human Pre-designed siRNA Set A-3-F	GAAGAAAGACAGUCGGUUUUU
LGALS3 Human Pre-designed siRNA Set A-3-R	AAACCGACUGUCUUUCUUCUU

qPCR). All cell lines were validated by short tandem repeat (STR) profiling and tested negative for mycoplasma.

2.8 Cell Proliferation

Cells of the PANC-1 and SW1990 lines that were in the logarithmic growth stage were seeded into 96-well plates at a cell concentration of 5×10^4 cells per milliliter, and each well was inoculated with 100 µL. After the cells adhere to the wall, each group of cells is provided with 5 multiple holes. Following a 48-hour treatment period, 10 µL Cell Counting Kit-8 (CCK-8) reagent was introduced into each well containing the complex, and then cultured in an incubator at 37 ° for 3 hours. After that, the 96-well plate was taken out, and an enzyme-labeled apparatus was employed to determine the value of the optical density (OD) at a wavelength of 450 nanometers and statistically analyzed. Cell survival rate = [(experimental hole absorbance-blank hole absorbance)/(control hole absorbance-blank hole absorbance)] × 100%.

2.9 Cell Migration

The logarithmic growth period PANC-1 and SW1990 cell lines were digested and diluted to create 5×10^6 cells per milliliter, which were then evenly distributed in the 6-well plates in 100 µL. At approximately 90% cell convergence, scratch with 200 µL gun head, cleaned with PBS, filled with culture medium, and imaged at 0, 24, and 48 hours, respectively.

2.10 RT-qPCR Analysis

The total RNA was isolated from HPDE6-C7, PANC-1, and SW1990 cells. Ultra-micro spectrophotometer (NanoDrop2000, Thermo Fisher Scientific, USA) was employed to measure the concentration of the total RNA. Subsequently, the total RNA was reverse-transcribed into complementary deoxyribonucleic acid (cDNA) using the PrimeScript™ RT reagent Kit with gDNA Eraser. Following the synthesis of cDNA, amplification was carried out, and the expression levels were measured with TB Green Premix Ex Taq II. The relative expression of the core genes was computed using the $2^{-\Delta\Delta Ct}$ method. The primer sequences are presented in Table 2.

2.11 Statistical Methods

The dataset was subjected to analysis using R project (version 4.4.2, Lucent Technologies, Murray Hill, New Jersey, USA), specifically version 4.3.1. For survival analysis, Kaplan–Meier survival analysis along with log-rank tests were employed. When dealing with variables, if a variable followed a normal distribution, the Student's *t*-test was selected for analysis. In cases where the variable did not conform to a normal distribution, the Wilcoxon test was utilized instead. To build the ROC curve, the "timeROC" package was applied. Across all investigations, statistical significance was defined as a *p*-value less than 0.05.

3. Results

3.1 DEGs Distinguishing Between Tumor and Normal Tissues

Through a comparison of the gene expression patterns of 26 tumor tissues and 26 normal tissues within the GSE16515 dataset, 2682 DEGs were identified (log2[fold change] >1, Q <0.05). A total of 1969 genes were upregulated in the tumor group, whereas 711 genes were downregulated (Fig. 1A). The GEPIA database yielded a total of 9222 DEGs in PC (log2[fold change] >1, Q <0.05), of which 481 were downregulated and 8741 were upregulated in tumor tissues (Fig. 1B). We obtained 17 NETosis-related DEGs (Fig. 1C) by constructing Venn diagrams to further investigate the relationships between these DEGs and NETosis-related genes. Following an initial screening of genes associated with survival via univariate cox regression analysis, eleven genes (*C5*, *CDC42*, *CXCL8*, *FN1*, *LGALS3*, *PLAUR*, *S100A11*, *DUOX2*, *SLC44A2*, *STAT1*, and *TNFSF10*) were pinpointed that met the criterion of $p < 0.05$ (Fig. 1D). LASSO regression analysis was conducted using the best λ value construction of six marker gene features (*FN1*, *STAT1*, *TNFSF10*, *SLC44A2*, *LGALS3*, *S100A11*; Fig. 1E,F).

3.2 Validation of the NETosis-Related Prognostic Model

A predictive gene model was established using the TCGA-PAAD dataset. The queue for the modeling was divided into groups with high and low risks based on the median of the risk score (Fig. 2A). A notable disparity in overall survival (OS) was evident between the low-risk and

Table 2. Primer sequences.

Primer name	Primer sequence
LGALS3-F	TTGCCTTCCACTTTAACCCAC
LGALS3-R	CCGACTGTCTTTCTTCCCTTC
S100A11-F	ACAGAACTAGCTGCCTTCACAAAGA
S100A11-R	GACAGAAAGGCTGGAAGGAAA
GAPDH-F	GGAAGCTTGTCATCAATGGAAATC
GAPDH-R	TGATGACCCTTTTGGCTCCC

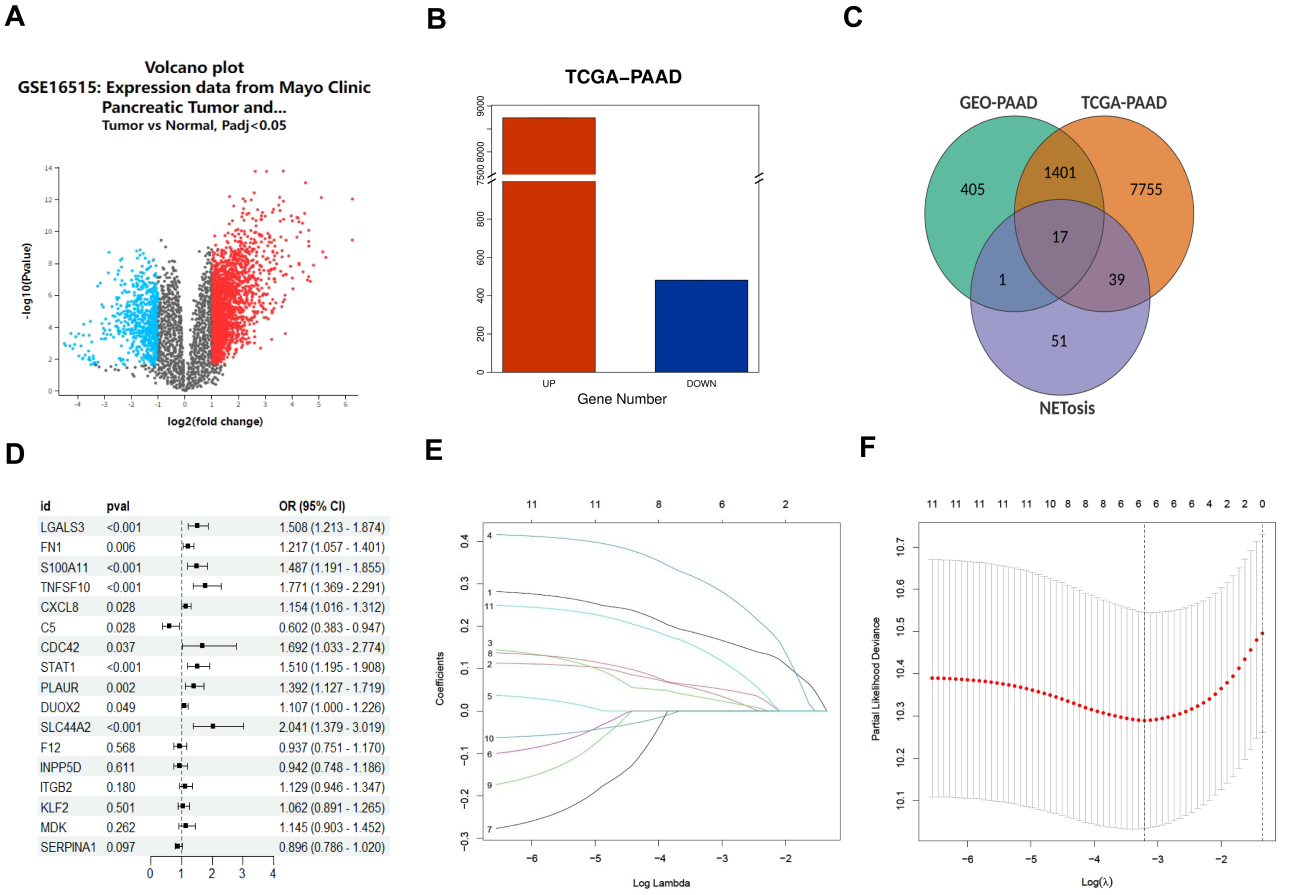

Fig. 1. Identification of neutrophil extracellular trap related genes signature. (A) Volcano plot of differentially expressed genes (DEGs) in GSE16515 dataset. (B) DEGs in The Cancer Genome Atlas - Pancreatic Adenocarcinoma (TCGA-PAAD) dataset. (C) Venn of neutrophil extracellular trap (NETosis) related DEGs. (D) Result of univariate Cox regression analysis, and 11 genes showed $p <$ 0.05. (E) The least absolute shrinkage and selection operator (LASSO) regression of the 11 genes associated with overall survival (OS). (F) LASSO regression parameter selection is tuned using cross-validation.

high-risk groups (p = 0.0159, Fig. 2B). Time-dependent ROC analysis was employed to evaluate the sensitivity and specificity of the prognostic model. The outcomes indicated that the area under the ROC curve (AUC) was 0.736 for 2-year survival, 0.792 for 3-year survival, and 0.872 for 4-year survival (Fig. 2C). Validation queues were derived from the GSE57495 dataset. Fig. 2D presents the dissemination of high- and low-risk classifications. Additionally, according to the Kaplan–Meier analysis, a significant difference in survival rates was detected between the high-risk and low-risk groups (p = 0.0263, Fig. 2E). The ROC curve for the validation dataset revealed that our model performed well in terms of prediction (0.698 for 2-year survival, 0.835 for 3-year survival, and 0.847 for 4-year survival; Fig. 2F).

3.3 Immunoinfiltration and Drug Susceptibility Analysis

We employed single-sample immune infiltration analysis (ssGSEA) to contrast the concentration scores of sixteen distinct types of immune cells and the activity degrees of thirteen immune-associated pathways between the high- and low-risk cohorts. In the TCGA dataset, it was shown that the high-risk cohort generally exhibited

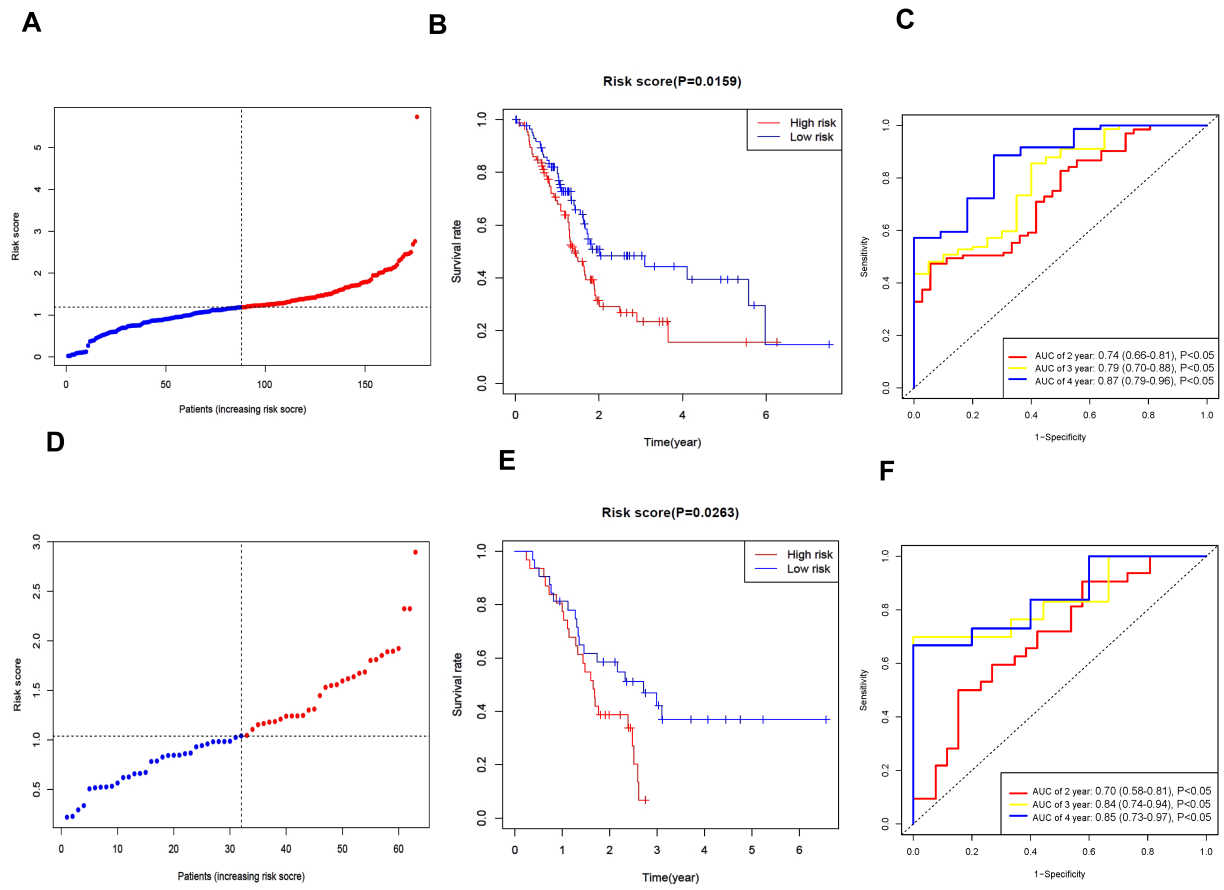

Fig. 2. Verification of the prognostic model associated with neutrophil extracellular trap. (A) Distribution of modeling queue based on the risk score. (B) The OS for modeling queue in the subunit is represented by Kaplan-Meier (KM) curve. (C) Receiver operating characteristic (ROC) curves of modeling queue. (D) Distribution of verification queue. (E) The OS for verification queue in the subunit is represented by KM curve. (F) ROC curves of verification queue. AUC, area under the ROC curve.

a greater abundance of activated dendritic cells (aDCs), macrophages, Th1 cells, and Treg compared to the low-risk cohort ($p < 0.05$, Fig. 3A). When conducting an analysis of the activities of immune-related pathways, it was found that in comparison to the low-risk cohort, the high-risk cohort exhibited a significantly higher level of enrichment for several pathways. These pathways include APC_co_inhibition, APC_co_stimulation, CCR, Check-point, HLA, Inflammation-promoting, MHC class I, Parainflammation, and Type IFN Response. The difference was statistically significant ($p < 0.05$), as shown in Fig. 3B. We also examined the sensitivity of subgroups to frequently used chemotherapeutic medications for PC, namely, 5-fluorouracil, gemcitabine, and epirubicin. The group at high risk demonstrated a greater degree of sensitivity to all three pharmaceutical agents compared to the group at low risk. ($p < 0.01$, Fig. 3C).

3.4 ScRNA Shows the Expression of Key Genes in Tumor Microenvironment Cell Clusters

Eight patients were included in the scRNA-seq dataset (Fig. 4A). A total of 49,056 genes and 6852 cells remained after removing some data with extremely low expression. Dimensionality reduction analysis was conducted using the t-SNE. Six cell clusters were identified (Fig. 4B). The bubble diagram's results demonstrate that each cell cluster's marker genes may be effectively distinguished (Fig. 4C). We used a t-SNE diagram to show the expression level of DEGs linked to NETosis in each cell cluster. The results demonstrated that epithelial cells exhibited high levels of *LGALS3* and *S100A11* (Fig. 4D). Since pancreatic cancer starts in epithelial cells, we speculate that these two genes have a crucial role in controlling the development and growth of tumor cells.

3.5 RT-qPCR and siRNA Interference Model

We verified the expression of *LGALS3* and *S100A11* in HPDE6-C7 and PANC-1 cells by RT-qPCR. The results demonstrated that pancreatic cancer cells had greater levels of *LGALS3*, and *S100A11* expression than normal pancreatic duct epithelial cells ($p < 0.05$, Fig. 5A). Findings from the survival analysis indicated that only pancreatic adenocarcinoma (PAAD) patients who exhibited elevated expression of the *LGALS3* gene experienced poorer overall

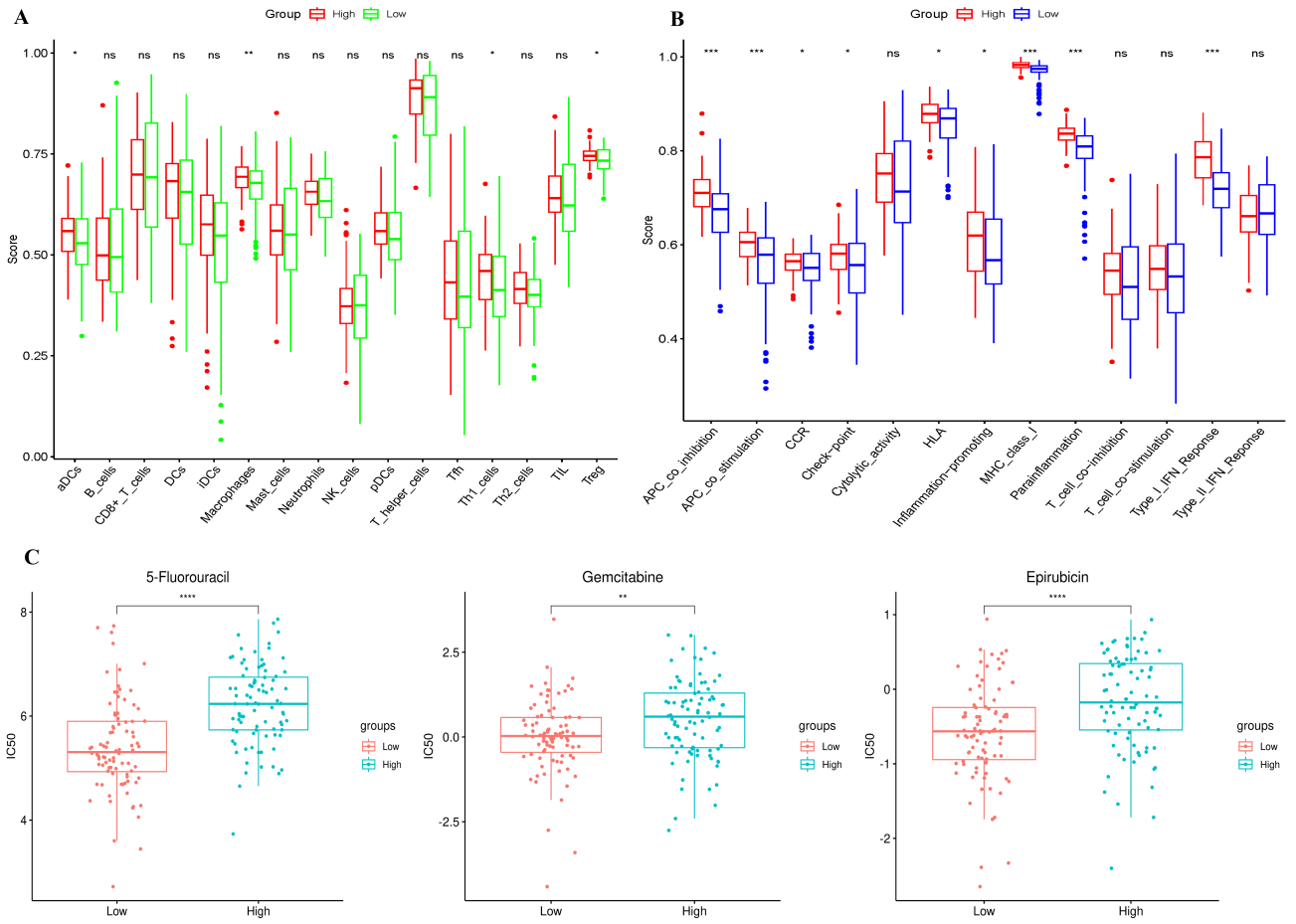

Fig. 3. Immunoinfiltration and drug susceptibility of subgroups. (A) In the TCGA cohort, a comparison was made of the enrichment scores of 16 distinct types of immune cells between subgroups. (B) In the TCGA cohort, a comparison was carried out regarding the enrichment scores of 13 immune-associated pathways between subgroups. (C) The sensitivity of the 5-fluorouracil, gemcitabine, and epirubicin in various risk groups. ns: $p > 0.05$; *: $p < 0.05$; **: $p < 0.01$; ***: $p < 0.001$; ****: $p < 0.0001$.

survival rates ($p < 0.05$, Fig. 5B). This result emphasizes the significance of *LGALS3* in pancreatic cancer, leading us to identify it as a critical gene and conduct an in-depth study into its mechanism. In order to explore the influence of *LGALS3* on the functionality of pancreatic cancer cells, we inhibited the expression of *LGALS3* in PANC-1 and SW1990 cells. After Sh-*LGALS3*-siRNA was transformed into PANC-1 and SW1990 cells, the total RNA was extracted and the interference efficiency was verified by RT-qPCR. The results demonstrated that the expression of *LGALS3* was significantly inhibited by the Sh-*LGALS3*-siRNA sequence ($p < 0.001$, Fig. 5C,D).

3.6 Interference With LGALS3 Expression Prevented PANC-1 and SW1990 Cells From Proliferating and Migrating

To further elucidate the mechanism by which *LGALS3* modulates pancreatic cancer cells, we assessed the proliferative activity and migratory capacity of two types of pancreatic cancer cells subsequent to transfection with siRNA. The outcomes of the Cell Counting Kit-8 (CCK8) assay indicated that the proliferative capacity of PANC-1 and SW1990 cells in the Sh-*LGALS3*-1, Sh-*LGALS3*-2, and Sh-*LGALS3*-3 groups was notably reduced compared to that in the Sh-*LGALS3*-NC group ($p < 0.05$, Fig. 6A,B). The results of the migration test demonstrated that interference with *LGALS3* markedly reduced the migrating capacity of PANC-1 and SW1990 cells ($p < 0.05$, Fig. 6C,D). Consequently, we verified that *LGALS3* is capable of triggering the dissemination and metastasis of pancreatic cancer by modulating the proliferation and movement of cancer cells.

4. Discussion

PC is a common type of malignant tumor. It shows rapid progression, a high mortality rate, and a poor prognosis. Recent studies have revealed that NETosis is an innovative form of cell death crucial for the development of malignancies and therapeutic approaches [13]. The tumor microenvironment releases neutrophil extracellular traps that shield tumor cells from cytotoxic immunity, thereby compromising tumor clearance. However, arteries also can be

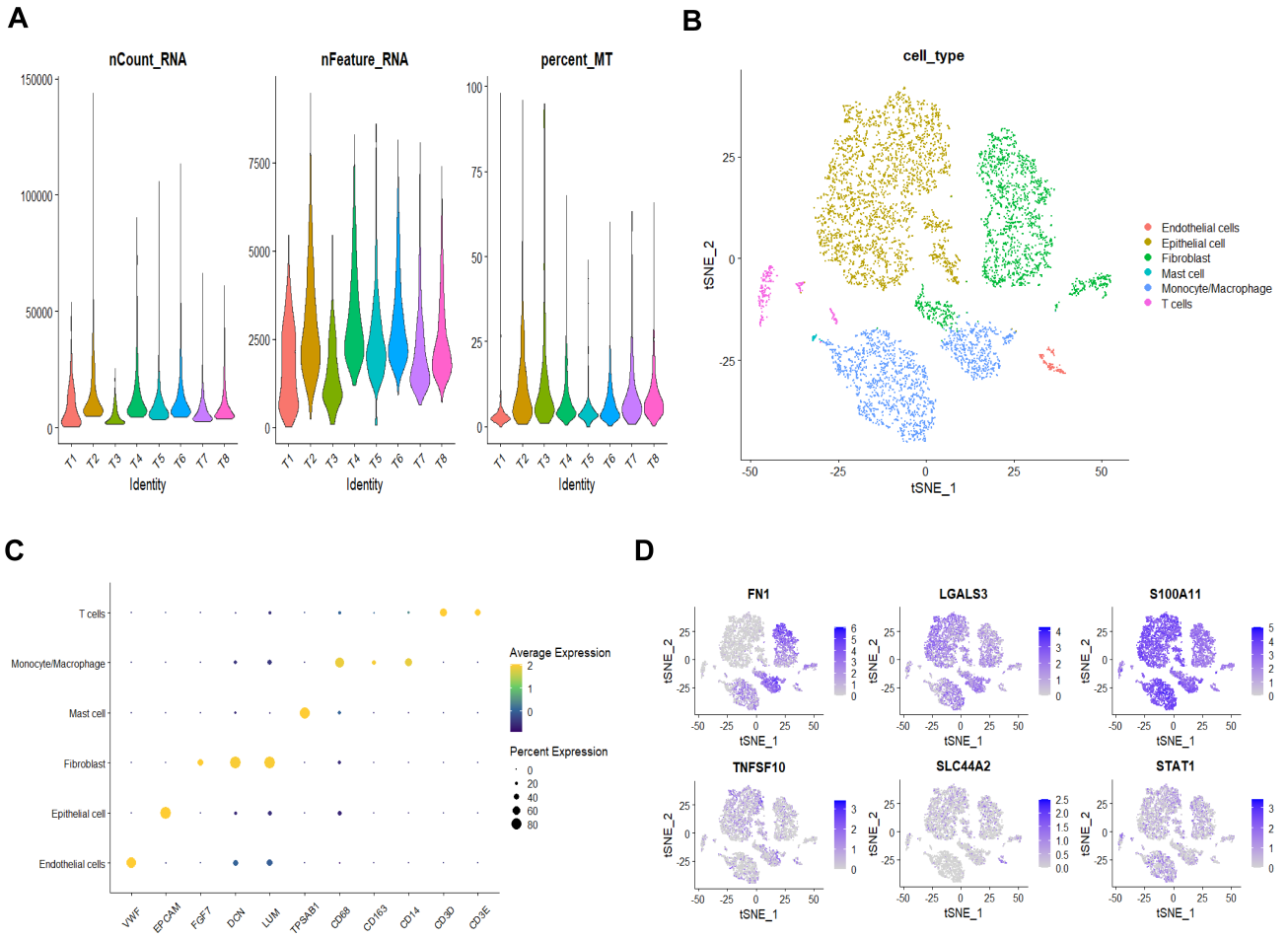

Fig. 4. Single cell analysis results of pancreatic carcinoma. (A) Quality control results for eight patients. (B) Six clusters were identified based on the dimensionality reduction of t-distributed stochastic neighbor embedding (t-SNE). (C) Bubble diagram showing each cell cluster's marker gene expression distribution. (D) The expression of NETosis-related DEGs in various cell clusters.

penetrated by tumor cells collected by neutrophil extracellular traps, which can then be seeded into distant organs [11]. In both PC and normal organizations, we initially acquired 17 DEGs associated with NETosis. Six genes (*FN1*, *STAT1*, *TNFSF10*, *SLC44A2*, *LGALS3*, and *S100A11*) prognosis models were created by LASSO, and their predictive value was assessed. NETosis-related gene features were identified in this study, offering theoretical support for further studies.

In malignant tumors, cell motility, epithelial–mesenchymal transition, and tight junctions between cells may be associated with NETosis. For instance, by activating m6A, the up-regulation of IGF2BP3 expression in malignant gliomas regulates the release of CSF3, causes NETosis, and subsequently stimulates tumor growth [17]. By attracting immune cells and increasing vascular permeability, Epithelial-Mesenchymal Transition (EMT) of malignant tumors also contributes to the development of NETosis, which causes distant areas to metastasize [18]. Furthermore, immune cells use a variety of mechanisms, including the production and release of NETosis, to take part in both innate and adaptive immune responses [19]. As a result, the process by which NETosis forms is complicated, and in addition to certain substances that the tumor itself releases, the immunological microenvironment is also crucial. Fibronectin 1 (*FN1*) is distributed across the extracellular matrix [20]. *FN1* has the ability to control signal transduction, migration, and cell adhesion [21]. By controlling inflammation and cancer cell motility, *FN1* can facilitate NETosis in the tumor microenvironment and facilitate contact with NETs, hence influencing the progression of cancer. In the nucleus, *STAT1* transduces signals from type I and type II interferons, serves as the primary mediator of the cellular response to interferons, and is a critical player in the immunological response [22]. Neutrophils with *STAT1* gain-of-function (GOF) mutations are young and highly activated, and they are highly susceptible to platelet-neutrophil aggregation, NETosis, and degranulation [23]. Apart from the tumor itself, *STAT1* activation affects the immunological milieu in a variety of ways. It can also indirectly cause NETosis by controlling inflammatory factors, which in turn influence

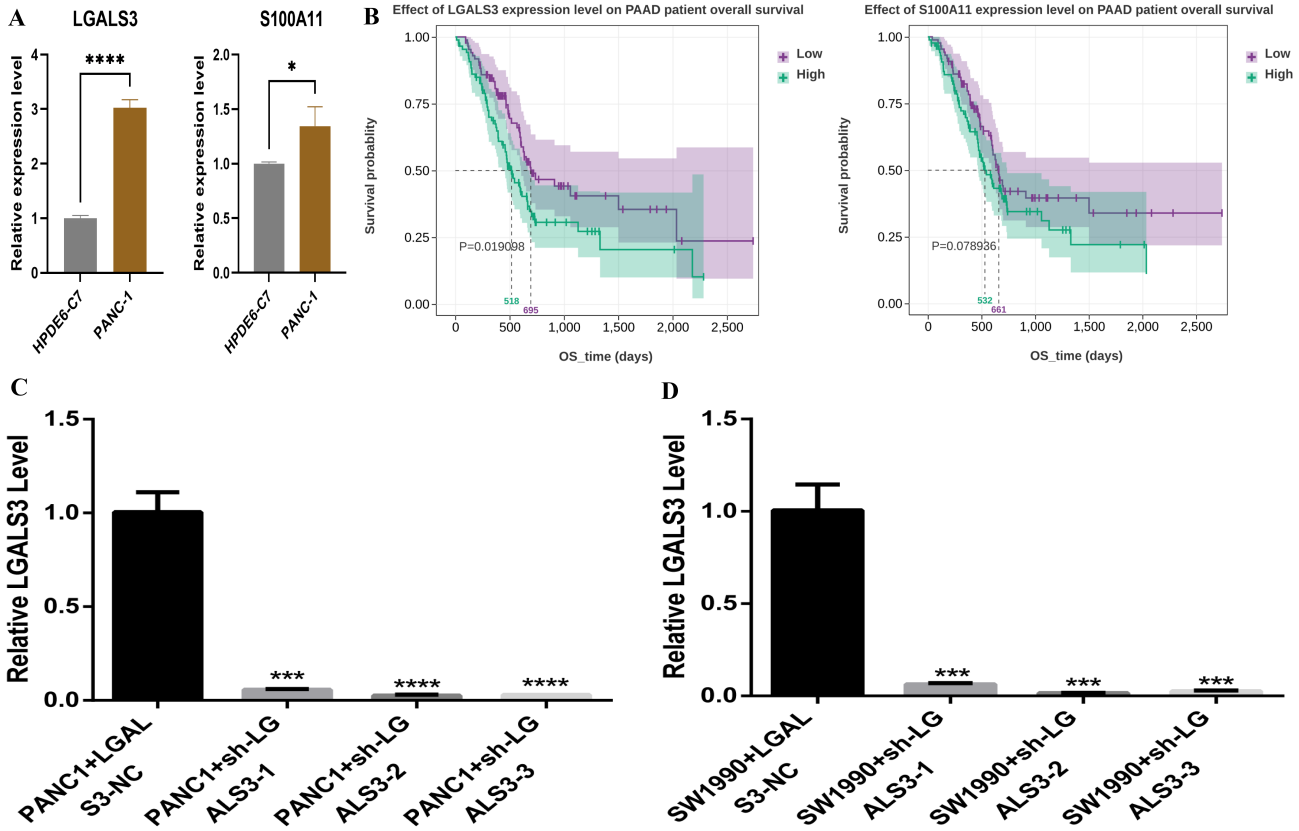

Fig. 5. Verification of *LGALS3* expression level. (A) Reverse Transcription Quantitative Real-Time Polymerase Chain Reaction verification of expression levels of *LGALS3* and *S100A11*. (B) Survival analysis of *S100A11* ($p = 0.019$) and *LGALS3* ($p = 0.079$). (C) Results of interference efficiency of PANC-1 cells. (D) Results of interference efficiency of SW1990 cells. *: $p < 0.05$; ***: $p < 0.001$; ****: $p < 0.0001$.

tumor growth [24]. *TNFSF10* is a factor responsible for tumor necrosis. It belongs to the tumor necrosis factor superfamily [25]. The "death receptor" *TNFSF10* is mostly expressed by immune cells. Apoptosis can be triggered and different cell activities can be controlled by activating these receptors [26]. By triggering associated signal pathways, *TNFSF10* can influence neutrophil activity and function, controlling NETosis and influencing the course of cancer. *SLC44A2*, the second member of solute carrier family 44, has been shown by Constantinescu-Bercu *et al.* [27] to mediate venous thromboembolism (VTE) and NETosis, and these two pathological conditions promote each other [28]. Substances released following platelet activation can activate neutrophils in the tumor microenvironment through receptors such as *SLC44A2*, forming a platelet–neutrophil complex and causing NETosis [29]. This has an impact on the angiogenesis, metastasis, and proliferation of tumor cells. Galectin 3 belongs to the family of proteins that bind to β-galactoside. It is released by a variety of immune cells as well as tumor cells. Galectin 3 promotes the growth, viability, and establishment of cancer cells via modulating the tumor microenvironment [30]. By attaching to relevant receptors, *LGALS3* may initiate signal pathways in malignancies. For instance, *HDAC7* can increase the production of *LGALS3* protein in gliomas via mediating SOX8/JUN axis signal transduction. It can then interact with tumor cell and immune cell membrane surface receptors via paracrine and autocrine pathways, respectively [31]. As a result, *LGALS3* can influence the immunological environment and NETosis by regulating immune system activity and the distinct phenotypic alterations of tumor cells. *S100A11* belongs to the S100 protein group and regulates angiogenesis, metastasis, cell proliferation, and immune evasion [32]. Research has demonstrated that NETosis can trigger the production of *S100A11* and further activate neutrophils to generate TNF and IL-6, hence intensifying the inflammatory response [33]. It is therefore crucial for the immune system and pancreatic cancer.

In summary, these six genes are crucial for regulating the immune system and the growth of tumors. Certain genes (including *LGALS3*, S100A11, etc.) can directly influence the migration and proliferation of tumor cells in addition to controlling the immunological milieu and the development of NETosis, which will have a significant impact on the prognosis of patients. Our research also verified that the

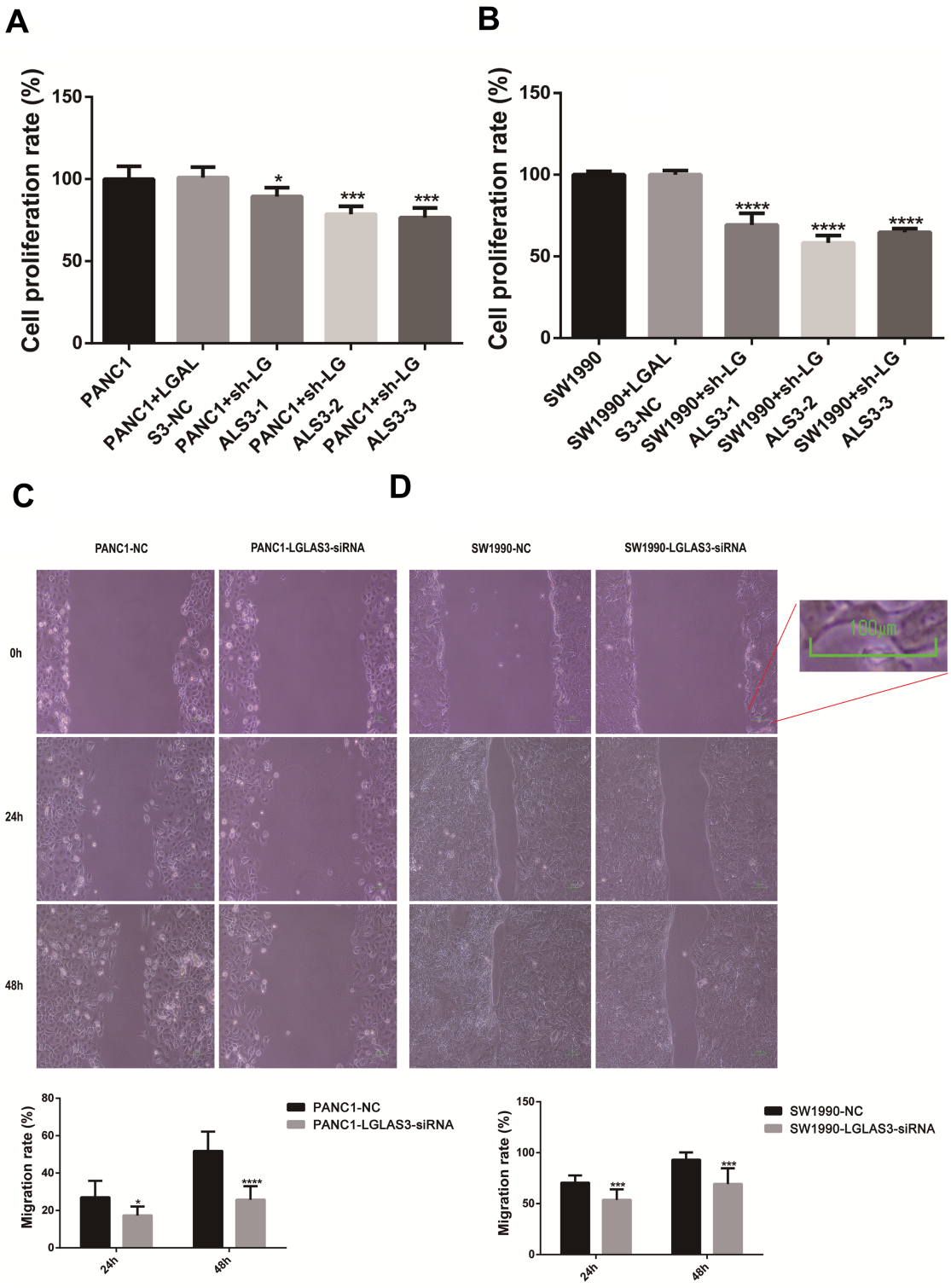

Fig. 6. Interference with *LGALS3* expression prevented PANC-1 and SW1990 cells from proliferating and migrating. (A) Cell Counting Kit-8 (CCK8) results of PANC-1 cells ($p < 0.05$). (B) CCK8 results of SW1990 cells ($p < 0.05$). (C) Results of migration of PANC-1 cells ($p < 0.05$), scale length: 100 µm. (D) Results of migration of SW1990 cells ($p < 0.05$), scale length: 100 µm. *: $p < 0.05$; ***: $p < 0.001$; ****: $p < 0.0001$.

two groups separated by this gene cluster had significantly different survival outcomes. Furthermore, we discovered that the immune cells in subgroups, which were separated by the prognostic model, differed considerably by the examination of immune infiltration: ADCs, macrophages, TH1 cells, Treg, and a variety of immunological activities,

including APC_co_inhibition, APC_co_stimulation, CCR and so on. These abnormal immunological processes may encourage tumor immune escape and alter medication sensitivity [34]. According to the results of our investigation, 5-fluorouracil, gemcitabine, and epirubicin may benefit the high-risk group, which will enhance the individualized and accurate treatment of more patients with pancreatic cancer.

Epithelial cells are the source of pancreatic cancer cells. The highly expressed genes (*LGALS3* and *S100A11*) in the tumor cells may be found by single-cell analysis. By combining RT-qPCR and survival analysis, we can find the crucial core gene *LGALS3*. Lastly, we used siRNA to disrupt *LGALS3* expression in PANC-1 and SW1990, and we discovered that the gene was crucial in controlling tumor migration and proliferation. These research results will assist in building gene detection assays in the future, predicting the outcome of patients suffering from PC during the initial phase, and providing novel treatment options to patients through focused intervention in the NETosis immune response.

There are some limitations to this study: (1) The magnitude of the sample in scRNA-seq data is extremely limited, and future efforts to expand the sample size are necessary. (2) The present study aims to reveal the relationship between NETosis and the occurrence and progression of pancreatic cancer, further investigation is required to determine the precise pathway of important genes.

5. Conclusion

In this research, a characteristic model involving six genes associated with NETosis was developed. This model exhibits excellent discriminatory capabilities and can offer guidance for the personalized and more precise treatment of high-risk populations. *LGALS3* has the ability to modulate the proliferation and migration of pancreatic cancer cells, subsequently triggering tumor progression. The identification of these genes holds the promise of serving as novel therapeutic targets for pancreatic cancer.

Availability of Data and Materials

The analyzed data sets generated during the study are available from the corresponding author on reasonable request.

Author Contributions

Conception and design: JXX, LYT, YC, LHJ. Provision of study materials and methodology: LHJ, JXX and LJM. Collection and assembly of data: JXX, LYT, LJM and QST. Data analysis and interpretation: YC, JXX and LYT. Manuscript writing: All authors. All authors have participated sufficiently in the work to take public responsibility for appropriate portions of the content and agreed to be accountable for all aspects of the work in ensuring that questions related to its accuracy or integrity. All authors read and approved the final manuscript. All authors contributed to editorial changes in the manuscript.

Ethics Approval and Consent to Participate

Not applicable.

Acknowledgment

Not applicable.

Funding

This research is supported by Yunnan Provincial Key Laboratory for Innovative Application of Traditional Chinese Medicine (202205AG070005), National Natural Science Foundation (82460095, 82460096) and Major scientific and technological projects in Yunnan Province (202402AA310006).

Conflict of Interest

The authors declare no conflict of interest.

References

[1] Javadrashid D, Baghbanzadeh A, Derakhshani A, Leone P, Silvestris N, Racanelli V, *et al*. Pancreatic Cancer Signaling Pathways, Genetic Alterations, and Tumor Microenvironment: The Barriers Affecting the Method of Treatment. Biomedicines. 2021; 9: 373. https://doi.org/10.3390/biomedicines9040373.

[2] Siegel RL, Miller KD, Wagle NS, Jemal A. Cancer statistics, 2023. CA: a Cancer Journal for Clinicians. 2023; 73: 17–48. https://doi.org/10.3322/caac.21763.

[3] Yamada T, Minami T, Yamada M, Terauchi Y. Proposed carbohydrate antigen 19-9 (CA19-9) cut-off values for the detection of pancreatic cancer in patients with poorly controlled diabetes: a real-world study. Endocrine Journal. 2023; 70: 1069–1075. https://doi.org/10.1507/endocrj.EJ23-0186.

[4] Li J, Li Y, Chen C, Guo J, Qiao M, Lyu J. Recent estimates and predictions of 5-year survival rate in patients with pancreatic cancer: A model-based period analysis. Frontiers in Medicine. 2022; 9: 1049136. https://doi.org/10.3389/fmed.2022.1049136.

[5] Jobu Y, Nishigawa M, Furihata K, Furihata M, Uchida K, Taniuchi K. Inhibitory effects of the combination of rapamycin with gemcitabine plus paclitaxel on the growth of pancreatic cancer tumors. Human Cell. 2025; 38: 44. https://doi.org/10.1007/s13577-024-01165-9.

[6] Zhang W, Zhang J, Liang X, Ding J. Research advances and treatment perspectives of pancreatic adenosquamous carcinoma. Cellular Oncology. 2023; 46: 1–15. https://doi.org/10.1007/s13402-022-00732-2.

[7] Ye X, Yu Y, Zheng X, Ma H. Clinical immunotherapy in pancreatic cancer. Cancer Immunology, Immunotherapy. 2024; 73: 64. https://doi.org/10.1007/s00262-024-03632-6.

[8] De Luca R, Gianotti L, Pedrazzoli P, Brunetti O, Rizzo A, Sandini M, *et al*. Immunonutrition and prehabilitation in pancreatic cancer surgery: A new concept in the era of ERAS® and neoadjuvant treatment. European Journal of Surgical Oncology. 2023; 49: 542–549. https://doi.org/10.1016/j.ejso.2022.12.006.

[9] Rizzo A, Mollica V, Tateo V, Tassinari E, Marchetti A, Rosellini M, *et al*. Hypertransaminasemia in cancer patients receiving immunotherapy and immune-based combinations: the MOUSEION-05 study. Cancer Immunology, Immunotherapy. 2023; 72: 1381–1394. https://doi.org/10.1007/s00262-023-03366-x.

[10] Di Federico A, Tateo V, Parisi C, Formica F, Carloni R, Frega G, *et al*. Hacking Pancreatic Cancer: Present and Future of Personalized Medicine. Pharmaceuticals. 2021; 14: 677. https://doi.org/10.3390/ph14070677.

[11] Hu Y, Wang H, Liu Y. NETosis: Sculpting tumor metastasis and immunotherapy. Immunological Reviews. 2024; 321: 263–279. https://doi.org/10.1111/imr.13277.

[12] Thiam HR, Wong SL, Wagner DD, Waterman CM. Cellular Mechanisms of NETosis. Annual Review of Cell and Developmental Biology. 2020; 36: 191–218. https://doi.org/10.1146/annurev-cellbio-020520-111016.

[13] Jaboury S, Wang K, O'Sullivan KM, Ooi JD, Ho GY. NETosis as an oncologic therapeutic target: a mini review. Frontiers in Immunology. 2023; 14: 1170603. https://doi.org/10.3389/fimmu.2023.1170603.

[14] Friedman J, Hastie T, Tibshirani R. Regularization Paths for Generalized Linear Models via Coordinate Descent. Journal of Statistical Software. 2010; 33: 1–22.

[15] Pérez JM, Martin PP. ROC curve. Semergen. 2023; 49: 101821. (In Spanish)

[16] Maeser D, Gruener RF, Huang RS. oncoPredict: an R package for predicting in vivo or cancer patient drug response and biomarkers from cell line screening data. Briefings in Bioinformatics. 2021; 22: bbab260. https://doi.org/10.1093/bib/bbab260.

[17] Dai W, Tian R, Yu L, Bian S, Chen Y, Yin B, *et al*. Overcoming therapeutic resistance in oncolytic herpes virotherapy by targeting IGF2BP3-induced NETosis in malignant glioma. Nature Communications. 2024; 15: 131. https://doi.org/10.1038/s41467-023-44576-2.

[18] Jinesh GG, Brohl AS. Classical epithelial-mesenchymal transition (EMT) and alternative cell death process-driven blebbishield metastatic-witch (BMW) pathways to cancer metastasis. Signal Transduction and Targeted Therapy. 2022; 7: 296. https://doi.org/10.1038/s41392-022-01132-6.

[19] Chamardani TM, Amiritavassoli S. Inhibition of NETosis for treatment purposes: friend or foe? Molecular and Cellular Biochemistry. 2022; 477: 673–688. https://doi.org/10.1007/s11010-021-04315-x.

[20] Bouvier C, Nihous H, Macagno N. Soft tissue tumours with FN1 (Fibronectin 1) fusion gene. Annales de Pathologie. 2022; 42: 242–248. (In French)

[21] Cai X, Liu C, Zhang TN, Zhu YW, Dong X, Xue P. Down-regulation of FN1 inhibits colorectal carcinogenesis by suppressing proliferation, migration, and invasion. Journal of Cellular Biochemistry. 2018; 119: 4717–4728. https://doi.org/10.1002/jcb.26651.

[22] Hossain MA, Larrous F, Rawlinson SM, Zhan J, Sethi A, Ibrahim Y, *et al*. Structural Elucidation of Viral Antagonism of Innate Immunity at the STAT1 Interface. Cell Reports. 2019; 29: 1934–1945.e8. https://doi.org/10.1016/j.celrep.2019.10.020.

[23] Parackova Z, Vrabcova P, Zentsova I, Sediva A, Bloomfield M. Neutrophils in STAT1 Gain-Of-Function Have a Pro-inflammatory Signature Which Is Not Rescued by JAK Inhibition. Journal of Clinical Immunology. 2023; 43: 1640–1659. https://doi.org/10.1007/s10875-023-01528-1.

[24] Lin S, Zhu P, Jiang L, Hu Y, Huang L, He Y, *et al*. Neutrophil extracellular traps induced by IL-1β promote endothelial dysfunction and aggravate limb ischemia. Hypertension Research. 2024; 47: 1654–1667. https://doi.org/10.1038/s41440-024-01661-3.

[25] Sag D, Ayyildiz ZO, Gunalp S, Wingender G. The Role of TRAIL/DRs in the Modulation of Immune Cells and Responses. Cancers. 2019; 11: 1469. https://doi.org/10.3390/cancers11101469.

[26] Cullen SP, Martin SJ. Fas and TRAIL 'death receptors' as initiators of inflammation: Implications for cancer. Seminars in Cell & Developmental Biology. 2015; 39: 26–34. https://doi.org/10.1016/j.semcdb.2015.01.012.

[27] Constantinescu-Bercu A, Grassi L, Frontini M, Salles-Crawley II, Woollard K, Crawley JT. Activated $\alpha_{IIb}\beta_3$ on platelets mediates flow-dependent NETosis via SLC44A2. eLife. 2020; 9: e53353. https://doi.org/10.7554/eLife.53353.

[28] Tavares V, Pinto R, Assis J, Pereira D, Medeiros R. Venous thromboembolism GWAS reported genetic makeup and the hallmarks of cancer: Linkage to ovarian tumour behaviour. Biochimica et Biophysica Acta. Reviews on Cancer. 2020; 1873: 188331. https://doi.org/10.1016/j.bbcan.2019.188331.

[29] Kenny M, Schoen I. A handshake between platelets and neutrophils might fuel deep vein thrombosis. Platelets. 2020; 31: 624–626. https://doi.org/10.1080/09537104.2020.1769053.

[30] Niang DGM, Gaba FM, Diouf A, Hendricks J, Diallo RN, Niang MDS, *et al*. Galectin-3 as a biomarker in breast neoplasms: Mechanisms and applications in patient care. Journal of Leukocyte Biology. 2022; 112: 1041–1052. https://doi.org/10.1002/JLB.5MR0822-673R.

[31] Zhao S, Zhao R, Wang C, Ma C, Gao Z, Li B, *et al*. HDAC7 drives glioblastoma to a mesenchymal-like state via LGALS3-mediated crosstalk between cancer cells and macrophages. Theranostics. 2024; 14: 7072-7087. https://doi:10.7150/thno.100939.

[32] Ji X, Qin X, Huang X, Wang W, Li H, Zheng C, *et al*. S100A11: A Potential Carcinogen and Prognostic Marker That Correlates with the Immunosuppressive Microenvironment in Pan-Cancer. Journal of Cancer. 2023; 14: 88–98. https://doi.org/10.7150/jca.78011.

[33] Navrátilová A, Bečvář V, Baloun J, Damgaard D, Nielsen CH, Veigl D, *et al*. S100A11 (calgizzarin) is released via NETosis in rheumatoid arthritis (RA) and stimulates IL-6 and TNF secretion by neutrophils. Scientific Reports. 2021; 11: 6063. https://doi.org/10.1038/s41598-021-85561-3.

[34] Maccalli C, Parmiani G, Ferrone S. Immunomodulating and Immunoresistance Properties of Cancer-Initiating Cells: Implications for the Clinical Success of Immunotherapy. Immunological Investigations. 2017; 46: 221–238. https://doi.org/10.1080/08820139.2017.1280051.